

# Synthesis and characterization of multi-lamellar mesostructured hydroxyapatites using a series of fatty acids

Jinhua Jiang · Yong Fan · Lirong Zhang ·  
Hong Yang · Yanli Chen · Dazhou Zhao ·  
Ping Zhang

Received: 18 September 2010 / Accepted: 17 January 2011 / Published online: 1 February 2011  
© Springer Science+Business Media, LLC 2011

**Abstract** A family of lamellar mesostructured hydroxyapatites are synthesized using five terminal linear aliphatic carboxylic acids (capric acid, lauric acid, myristic acid, palmitic acid, and stearic acid with the general formula of  $C_{n-1}H_{2n-1}CO_2H$ ,  $n = 10, 12, 14, 16, 18$ ). The study of X-ray diffraction shows that the hydroxyapatite samples exhibit similar multi-lamellar mesostructure and their interlamellar spacing is proportional to the carbon numbers of carboxylic acids. The transmission electron microscopic images on the products prove the parallel aligned configuration. Fourier transform infrared spectra displays the characteristic components of hydroxyapatite in as-prepared samples. Thermogravimetric analysis, elemental analysis (C, H), and inductively coupled plasma analysis were further used to confirm the organic and inorganic composition of the products.

## Introduction

Hydroxyapatite (HA,  $Ca_{10}(PO_4)_6(OH)_2$ ), the prime constituent of tooth and bone mineral [1, 2], is traditionally used as substitution for bone and dental materials because of its biocompatibility and bioactivity [3–6]. In the latest decades, owing to its various surface properties of surface

functional groups, acidity and basicity, surface charge, hydrophilicity and porosity, HA has been highlighted in extensive applications such as catalyst in chromatography, gas sensor, fertilizer production, water purification, and medical treatment like targeted and controlled drug delivery systems [7–11]. The present and potential applications of HAs are stimulating research efforts on the structural control on the nanometer scale.

Recently, lamellar materials have received considerable attention for their changeable layer constituent and adjustable interlamellar spacing owing to its varieties of interlamellar inorganic or organic functional ions [12–17]. Especially, layered materials with mesoscale interlayer spacing such as layered double hydroxides and mixed-metal oxides have demonstrated their applications as catalysts, drug carriers, and materials for separation of organic isomers [18–23]. As a result, the study of bioactive HAs with lamellar mesostructure may provide possibilities for the applications in catalysis, adsorption, medical treatment, etc.

The introduction of surfactants is desirable to have effective control on the mesostructures of calcium phosphate system, including hydroxyapatite [24–29]. To the synthesis of mesoporous calcium phosphates, several kinds of nonionic and amphiphilic surfactants have been adopted. Nonionic surfactants, such as F127 (EO99PO65EO99) and P123 (EO20PO70EO20), were applied in the assembly of high surface area mesoporous calcium phosphate particles with  $S_{BET} > 200 \text{ m}^2/\text{g}$  [24]. The combination of sodium dodecyl sulfate (SDS) with a soluble metal salt and a phenylphosphonic acid solution led to the production of mesoporous calcium phosphates with improved thermal stability [25]. Using surfactants hexadecylamine ( $C_{16}H_{33}NH_2$ ), and hybrid templates of mono-*n*-dodecyl phosphate ( $(C_{12}H_{25}O)P(O)(OH)_2$ , MDP) and cetyltrimethylammonium bromide (CTAB), mesostructured lamellar

**Electronic supplementary material** The online version of this article (doi:10.1007/s10853-011-5297-y) contains supplementary material, which is available to authorized users.

J. Jiang · Y. Fan · L. Zhang · H. Yang · Y. Chen · D. Zhao ·  
P. Zhang (✉)  
Department of Chemistry, Key Laboratory of Inorganic  
Synthesis and Preparative Chemistry, Jilin University,  
130012 Changchun, China  
e-mail: zhangping@jlu.edu.cn

calcium phosphates with different morphologies of hollow vesicle [26], micron-sized rods and short fiber [27] were obtained. The *n*-hexadecylamine was also used to synthesize a lamellar mesostructured calcium phosphate in the water–ethanol system by Ikawa et al. [28]. Lamellar octacalcium phosphates (OCP) was produced in the presence of dicarboxylate ions ( $^-\text{OOC}(\text{CH}_2)_n\text{COO}^-$ ) [29].

Nowadays, synthesis of HAs with mesostructure has attracted much attention in the chemistry and materials communities. The familiar cationic surfactant CTAB was used to synthesize mesoporous hydroxyapatite by Yao et al. in 2003 [30]. In 2005, under different concentrations of pluronic F127, two mesoporous hydroxyapatites with a maximum distribution of pore size 58 Å and bimodal pore size distribution at 25.3 or 30 Å were observed [31]. Another pluronic Tween-60 (polyoxyethylene (20) sorbitan monostearate) was successfully employed to synthesize lamellar hydroxyapatite with worm-like mesopores by Guo and Zhang [32]. Recently, with the existence of CTAB, Coelho et al. [33] reported their research on the effects of the sintering temperature on the morphological and crystallographic characteristics and on chemical composition of the “as-prepared” mesoporous hydroxyapatite. In the latest years, many kinds of anionic surfactants were exploited to produce lamellar mesostructured hydroxyapatite. The first attempts via reaction of alkyl phosphates with calcium inorganic source to prepare lamellar mesostructured hydroxyapatite went back to the groups of Ozin, Tanaka, Ostafin, etc., [4, 34, 35]. Their synthetic strategy is based upon the surfactant cooperative assembly of a calcium alkylphosphate lamellar phase and a calcium hydroxyphosphate (CaP) mineral phase. Later, phosphoric acid monododecyl ester (MAP) [36] and sodium dodecyl sulfate (SDS) [37] were introduced into the preparation of highly ordered mesolamellar hydroxyapatite in water–ethanol solution. In 2008, three more mesolamellar hydroxyapatites were reported by Ikawa’s group using *n*-hexadecanethiol, *N*-lauroyl-*L*-glutamic acid, and palmitic acid surfactants [38]. They discussed the interaction between ionic surfactants and calcium phosphates and subsequently the influence of surfactants to final Ca/P molar ratio.

Alcohol, as a cosolvent, is an important factor for the formation of lamellar mesostructured calcium phosphates. Ikawa et al. [28, 38, 39] have developed the synthetic method of lamellar mesostructured calcium phosphate in the mixed solvent system of ethanol and water, which suppresses the crystallization and controls the solubility of calcium phosphate species. In the two groups of Zhang and Liu, [36, 37] lamellar mesostructured hydroxyapatites were prepared with the presence of ethanol. It was pointed out that amorphous materials and inexistence of HA mesostructured phase occurred when there was no ethanol in the experiments [36].

Up to now, to the best of the understanding, fatty acids have rarely been applied to produce mesostructured hydroxyapatite, and the research on adjusting interlamellar spacing by terminal linear aliphatic carboxylic acids has not been reported. In this article, the authors synthesized highly ordered lamellar mesostructured HAs using five terminal linear aliphatic carboxylic acids with different alkyl chain lengths (capric acid, lauric acid, myristic acid, palmitic acid, and stearic acid with the general formula of  $\text{C}_{n-1}\text{H}_{2n-1}\text{CO}_2\text{H}$ ,  $n = 10, 12, 14, 16, 18$ ) in EtOH/H<sub>2</sub>O system by molecular self-assembly method. By means of TEM and XRD techniques, the structures of products are found to be similar multi-lamellar mesostructure. The authors also investigated the relation of the anion chain length and the interlamellar spacing of the products and proved that the interlamellar spacings are proportional to the carbon numbers of carboxylic acids. The result indicates that the interlayer spacing of HAs can be controlled and HAs with suitable interlayer spacing can be provided to accommodate functional molecules for further applications.

## Experimental section

### Materials

Calcium nitrate ( $\text{Ca}(\text{NO}_3)_2 \cdot 4\text{H}_2\text{O}$ ), ammonium hydrogen phosphate ( $(\text{NH}_4)_2\text{HPO}_4$ ), capric acid, lauric acid, myristic acid, palmitic acid, and stearic acid, sodium hydroxide (NaOH), absolute alcohol and deionized water. All chemicals were analytical grade and used as received without further purification.

### Sample preparation

In the preparation, all preparation of products were performed in ethanol–water solution containing 50% ethyl alcohol and 50% water (in volume). In a typical synthesis, 18.80 mmol of aliphatic carboxylic acid and 25.00 mmol of  $\text{Ca}(\text{NO}_3)_2 \cdot 4\text{H}_2\text{O}$  were mixed in 30 mL of the ethanol–water solution during constant stirring at 37 °C. Then 15.00 mmol of  $(\text{NH}_4)_2\text{HPO}_4$  (Ca/P = 10/6, molar ratio) in 30 mL ethanol–water solution was added. After further stirring for half an hour, 20 mL of 2 M NaOH ethanol–water solution was slowly added. The mixture was stirred at 37 °C for another 4 h. The final pasty suspension with a pH of 10 was transferred into a Parr Teflon-lined stainless steel vessel (100 mL) and heated at 100 °C for 24 h. The five samples H1, H2, H3, H4, and H5, corresponding to capric acid, lauric acid, myristic acid, palmitic acid, and stearic acid, respectively, were obtained after filtering,

washing thoroughly with hot water and ethanol, and drying at room temperature.

### Characterization

Powder X-ray diffraction (XRD) data were obtained using SHIMADAZU XRD-6000 diffractometer with Cu-K $\alpha$  radiation ( $\lambda = 1.5418 \text{ \AA}$ ). Fourier transform infrared (FTIR) spectra were recorded in the range of 400–4000  $\text{cm}^{-1}$  on a Nicolet 5PC FT-IR spectrophotometer using KBr pellets method. Thermogravimetric analysis (TG) was conducted for thermal behaviors of the as-prepared samples on a SHIMADAZU DTG 60 thermogravimetric analyzer with a heating rate of 10  $^{\circ}\text{C min}^{-1}$  in air up to 800  $^{\circ}\text{C}$ . Inductively coupled plasma (ICP) analysis was performed on a Perkin-Elmer Optima 3300DV spectrometer. Elemental analyses were conducted on a Perkin-Elmer 2400 elemental analyzer. Field-emission scanning electron microscopy (FESEM) images were obtained with a XL30 ESEM FEG microscope fitted with an Oxford LINK EDS analyzer. Transmission electron microscopic (TEM) studies were carried out on a HITACHI H-8100 electron microscope with an acceleration voltage of 200 kV.

## Results and discussion

### Effect of EtOH/H<sub>2</sub>O volume ratio

In order to investigate the optimal ratio of EtOH/H<sub>2</sub>O, the synthesis using palmitic acid was carried out in the mixed solvent with volume ratios of EtOH/H<sub>2</sub>O of 0:100, 25:75, 40:60, 50:50, 60:40, and 75:25 in the same procedure in sample preparation. The XRD patterns of the products prepared with different volume ratios of EtOH/H<sub>2</sub>O are shown in Fig. 1. When the preparation was performed in EtOH/H<sub>2</sub>O of 0:100, and 25:75, impurity appeared in products (Fig. 1). With the increase of amount of EtOH in EtOH/H<sub>2</sub>O of 40:60, 50:50, 60:40, and 75:25, the peaks due to impurity disappeared. Thus, it was chosen the optimal volume ratio of EtOH/H<sub>2</sub>O of 50:50 in the following synthesis.

### Structure, morphology and formation of the samples synthesized using five fatty acids

The small and wide-angle X-ray diffraction patterns of the five samples (H1, H2, H3, H4, and H5) are shown in Fig. 2. The small-angle X-ray diffractions ( $2\theta < 10^{\circ}$ ) (Fig. 2a) are

**Fig. 1** The small (a) and wide-angle (b) X-ray diffraction patterns of the products prepared in the mixed solvent with different volume ratios of EtOH to H<sub>2</sub>O using palmitic acid (\* impurity)

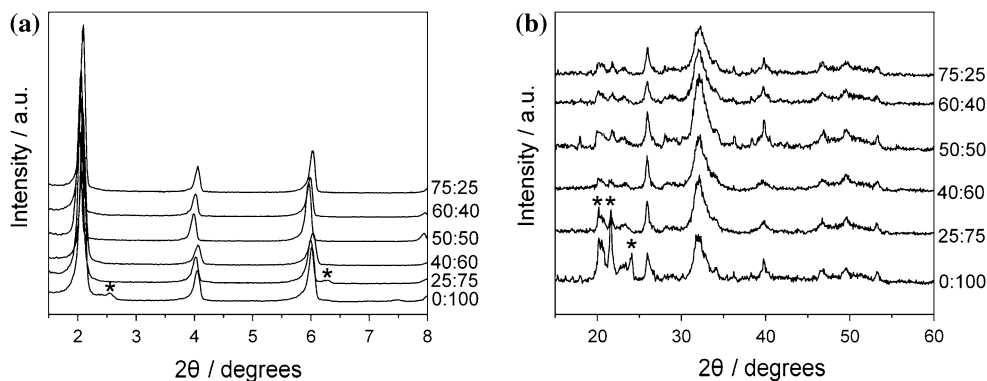
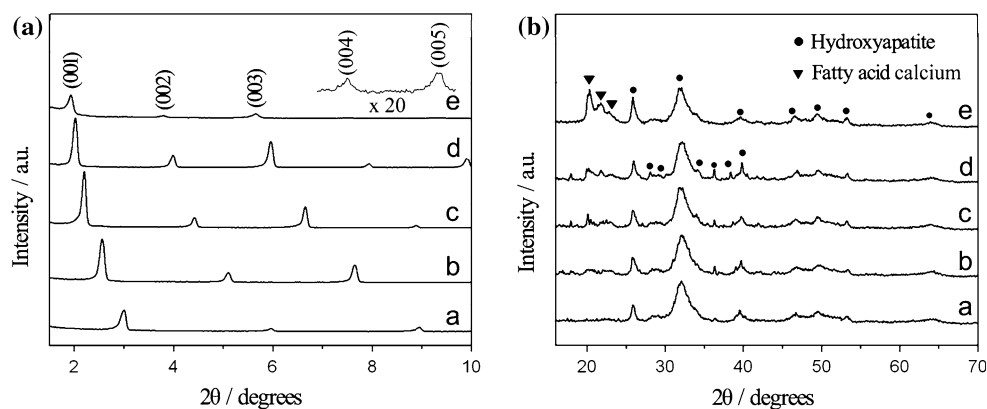


**Fig. 2** The small (a) and wide-angle (b) X-ray diffraction patterns of five products (a H1, b H2, c H3, d H4, e H5) prepared with capric acid, lauric acid, myristic acid, palmitic acid, and stearic acid, respectively



labeled by (001), (002), (003), (004), and (005), respectively. The structure style can be identified by Bragg's equation:  $2d \sin\theta = \lambda$ , where  $\lambda = 1.5418 \text{ \AA}$ ,  $d$  is the interplanar spacing and  $\theta$  is the Bragg angle. All the small-angle diffraction data are showed in Table 1. The calculation of  $d$  spacing ratio of the samples gives close to 1:1/2:1/3 for H1 and H2, 1:1/2:1/3:1/4 for H3, and 1:1/2:1/3:1/4:1/5 for H4 and H5. Compared with the references [37, 40], the small-angle pattern of the five samples suggests that long-range ordered layered mesostructured products are formed with a periodical spacing of 29.7, 34.5, 40.2, 43.7, and 45.8 Å for H1, H2, H3, H4, H5, respectively. In order to investigate the influence of surfactants on the ordered mesostructure, sample H0 without fatty acid was prepared as a comparison. H0 does not show any peaks in small-angle diffraction region and its wide-angle diffraction patterns coincides well with the standard data for hydroxyapatite (JCPDS no. 09-0432) in Fig. S1. This result demonstrates fatty acid is necessary for the formation of mesostructured HA as structure-directing agents. On the basis of the result of elemental analysis, ICP and TG (Fig. S2), the molar compositions of acid:Ca:P of the five products are 0.26:1.68:1, 0.30:1.68:1, 0.31:1.70:1, 0.52:1.71:1, and 0.41:1.72:1, corresponding to  $C_{n-1}H_{2n-1}CO_2H:CaO:1/2P_2O_5$  ( $n = 10, 12, 14, 16, 18$ ).

For the wide-angle diffraction patterns of products, shown in Fig. 2b, most of reflections are in agreement with

JCPDS no. 09-0432 displaying the peaks of HA; and the peaks are broad and of low intensity indicating that inorganic layers of HA are at a low level of crystallization. Jack and Vallet-Regí [41, 42] also found that the incorporation of the amino acids increased the fraction of amorphous material in the particles. They explained that the presence of organic acids in solution significantly reduces the kinetics of crystallization of HA from a supersaturated solution onto seed particles, which leads to a broad featureless peak in XRD pattern. For H3, H4, and H5, three more diffraction peaks found at 20.1°, 21.8°, and 22.8° can be assigned to the reflections of fatty acid calcium (JCPDS 05-0007, 09-0851, 09-0852, 05-0012, 05-0010). The molar ratio of Ca:P from ICP analyses on H1, H2, H3, H4, and H5 are 1.68:1, 1.68:1, 1.70:1, 1.71:1, and 1.72:1, respectively, which are close but little higher than that of hydroxyapatite (1.67). It implies that the amount of fatty acid calcium is quite small, for H1 and H2, it even can not be detected by XRD analysis.

The TEM images (Fig. 3) of H1, H2, H3, H4, and H5 further display the black-and-white stripe photograph which reveals the lamellar structure with alternating layers of fatty acids (white) and HA phase (black). The periodic spacing of the layers of 31.7, 36.9, 42.0, 45.6, and 46.8 Å, corresponding to samples H1, H2, H3, H4, and H5, respectively, are accordant to the values of 29.7, 34.5, 40.2, 43.7, and 45.8 Å from XRD analysis. TEM and XRD researches on the five samples show that the more the carbon numbers of the fatty acids, the larger the interlamellar spacing of the products. This result indicates that the interlamellar spacing of the products can be controlled by chain length of fatty acids.

The FTIR spectra of the fatty acids-HA series are shown in Fig. 4, and the assignment of bands is summarized in Table 2 [43, 44]. Phosphate absorption bands occurring at 1113, 1030, 956, 604, and 560  $cm^{-1}$ , and the hydroxide absorption band at about 3570  $cm^{-1}$  (marked with arrows), are representative peaks of hydroxyapatite. The existence of the antisymmetric stretching band (2919  $cm^{-1}$ ) and the symmetric stretching band (2851  $cm^{-1}$ ) of  $CH_2$  groups (abbreviated  $\nu_{as}(CH_2)$  and  $\nu_s(CH_2)$ , respectively) illuminates that the  $n$ -alkyl chains of the fatty acids possess an ordered all-trans conformation in the interlayer space which is important for the following discussion of the formation procedure of HAs. According to references [45–48], the bands at  $\sim 2920$  and  $2850 \text{ cm}^{-1}$  are sensitive to  $n$ -alkyl chain conformation and both of the bands will shift to higher wavenumbers if disorder (kink and gauche-blocks) is introduced into the  $n$ -alkyl chains.

The assumption of the formation of HAs

A linear relationship between the number of carbon atom  $n_c$  of the fatty acids and the basal space  $d_{001}$  of five lamellar

**Table 1** Small-angle X-ray diffraction data of the five mesostructured hydroxyapatites

Sample	$2\theta(^{\circ})$	$n$	$d$ (nm)	$nd$ (nm)	(hkl)
H1	3.00	1	29.7	29.7	001
	5.96	2	14.8	29.6	002
	8.96	3	9.9	29.7	003
H2	2.56	1	34.5	34.5	001
	5.10	2	17.3	34.6	002
	7.66	3	11.5	34.5	003
H3	2.20	1	40.2	40.2	001
	4.42	2	20.0	40.0	002
	6.66	3	13.3	39.9	003
	8.88	4	10.0	40.0	004
H4	2.02	1	43.7	43.7	001
	3.99	2	22.1	44.2	002
	5.97	3	14.8	44.4	003
	7.95	4	11.1	44.4	004
	9.92	5	8.9	44.5	005
H5	1.93	1	45.8	45.8	001
	3.80	2	23.2	46.4	002
	5.66	3	15.6	46.8	003
	7.52	4	11.7	46.8	004
	9.38	5	9.4	47.0	005

**Fig. 3** The TEM images of five hydroxyapatites (*a* H1, *b* H2, *c* H3, *d* H4, *e* H5)

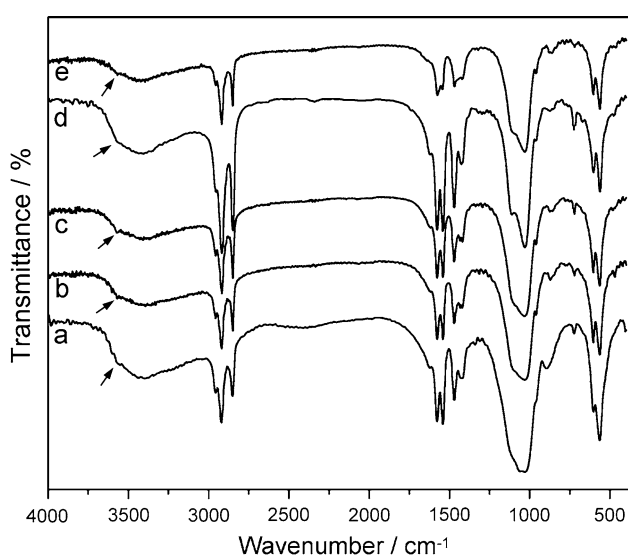
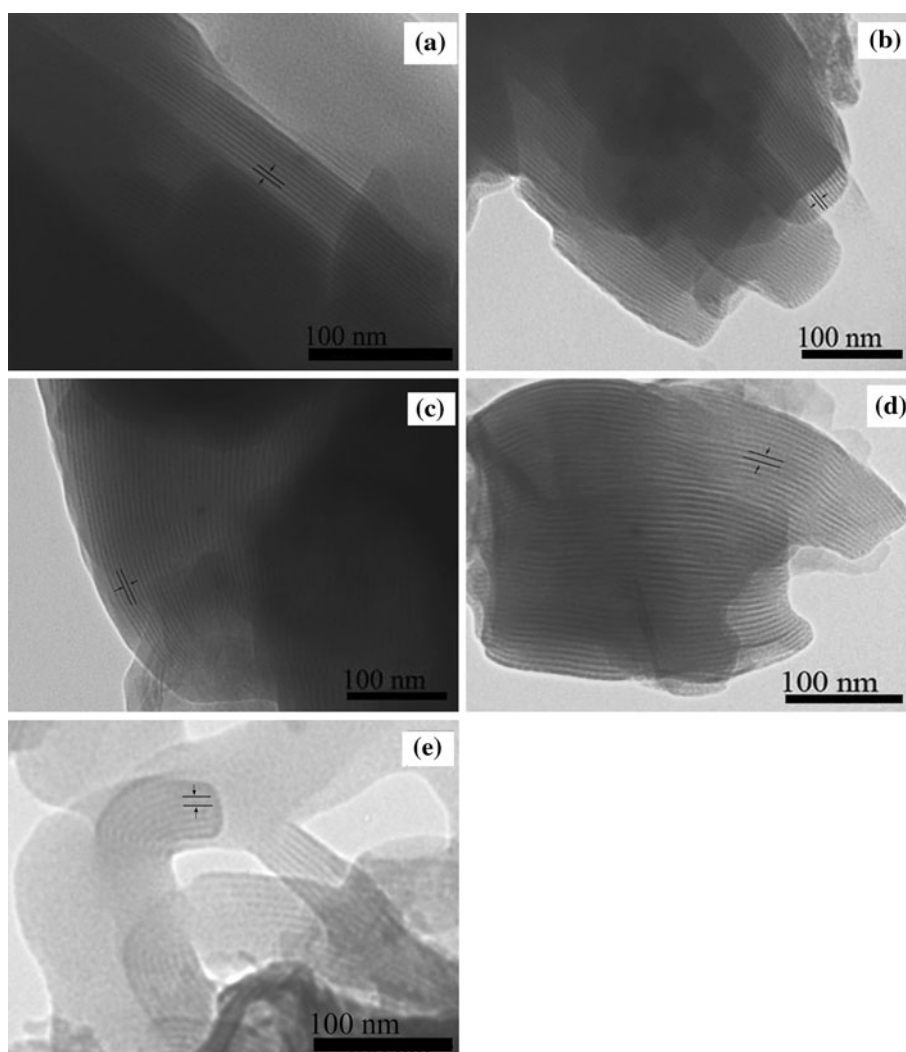


**Fig. 4** FTIR spectra of five hydroxyapatites (*a* H1, *b* H2, *c* H3, *d* H4, *e* H5)

HAs (H1, H2, H3, H4, and H5) is obtained from XRD data (Fig. 5), as expressed with  $d_1 = 2.07 n_c + 9.80$ , which means the interlamellar spacing is proportional to the chain length. Because the mean increment of the basal spaces ( $\Delta d/\Delta n_c$ ) is  $2.07 \text{ \AA}$ , which is larger than  $1.27 \text{ \AA}/\text{CH}_2$  for an all-*trans* fully extended alkyl chain [49], the alkyl chains might be arranged as bilayers in the interlayer region with a tilt angle of  $\sin^{-1}[2.07/(2 \times 1.27)]$ , i.e.,  $54.6^\circ$ . The intercept for  $n_c = 0$  (about  $9.80 \text{ \AA}$ ) is the average thickness of the HAs layer which is acceptable, because the value is close to that of  $11.2, 10.5, 12.9, 13.0,$  and  $12.5 \text{ \AA}$  (H1, H2, H3, H4, H5) obtained from TEM images.

The organization of surfactants and inorganic molecular species to produce two-dimensional periodic biphasic arrays has been described by Huo et al. [50] as the cooperative templating model, which has been accepted widely in the research of materials with mesostructures. Following their point of view, the authors try to presume a reaction process

**Table 2** Tabulated IR Spectrum of the five mesostructured hydroxyapatites

Wavenumber (cm <sup>-1</sup> )	Assignment	Source
3,570	$\nu_s$ (OH)	Hydroxyapatite
3,404	$\nu_s$ (OH)	Solvent (H <sub>2</sub> O, ethanol)
2,958	$\nu_s$ (CH <sub>3</sub> )	Fatty acid
2,919	$\nu_{as}$ (CH <sub>2</sub> )	Fatty acid
2,852	$\nu_s$ (CH <sub>2</sub> )	Fatty acid
1,583	$\nu_{as}$ (COO)	Fatty acid
1,541	$\nu_{as}$ (COO)	Fatty acid
1,468	$\nu_s$ (COO)	Fatty acid
1,426	$\delta$ (CH <sub>3</sub> ); $\nu$ (C–C) + $\rho$ (OCO)	Fatty acid
1,113	$\nu$ (PO <sub>4</sub> <sup>3-</sup> )	Hydroxyapatite
1,030	$\nu$ (PO <sub>4</sub> <sup>3-</sup> )	Hydroxyapatite
956	$\nu$ (PO <sub>4</sub> <sup>3-</sup> )	Hydroxyapatite
720	$\delta$ (CH)	Fatty acid
604	$\nu$ (PO <sub>4</sub> <sup>3-</sup> )	Hydroxyapatite
560	$\nu$ (PO <sub>4</sub> <sup>3-</sup> )	Hydroxyapatite

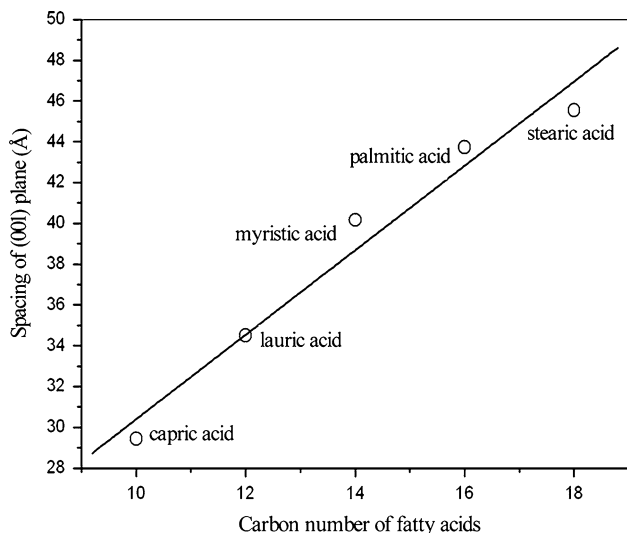


**Fig. 5** Relation between the carbon number of fatty acids and spacing of (001) plane of five products

of the mesostructured HAs as bellow (Fig. 6). At the initial time of the experiments, anionic aliphatic carboxylic acid reacted with cationic Ca<sup>2+</sup> ion through electrostatic interaction. After the addition of phosphate ions and OH<sup>-</sup>, inorganic tricalcium phosphate, without hydrothermal treatment, was formed and the rearrangement of fatty acids-tricalcium phosphate occurred simultaneously according to the anion charge density and shape requirements [50]. As a result, a lamellar mesostructured tricalcium phosphate was obtained which was confirmed by the small- and wide-angle

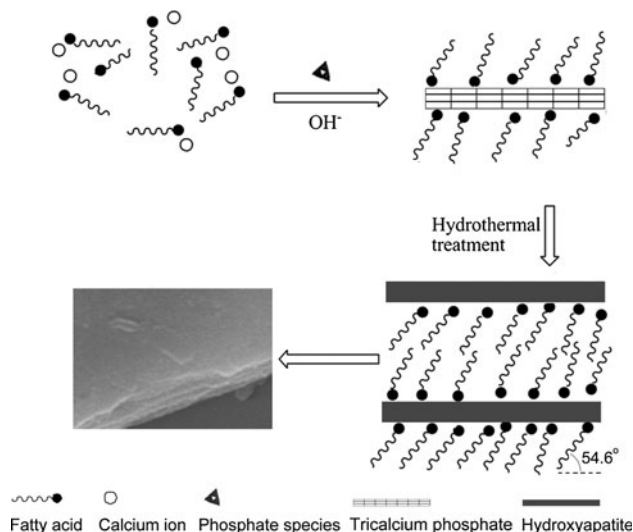


**Fig. 6** Schematic formation mechanism of the ordered lamellar hydroxyapatites (inseting photo supplied from Fig. S3)

XRD analysis in Fig. S4. After the hydrothermal treatment, the inorganic calcium phosphate was transformed into hydroxyapatite phase meanwhile kept the lamellar mesostructure which was also confirmed by XRD analysis (Fig. S4). Consequently, products with lamellar mesostructure were constructed with the alternate array of organic surfactant bilayers and the inorganic hydroxyapatite.

**Conclusion**

The authors successfully synthesized five multi-lamellar mesostructured hydroxyapatites, of which the alternating layers of fatty acids and HA phases are organized as a multilayer lamella. The possible formation process of multi-lamellar hydroxyapatites with mesostructure was presented. The study on the structure of the products indicates that interlamellar spacing is proportional to the chain length of fatty acids. The multi-lamellar mesostructured hydroxyapatites with changeable interlayer spacings might be a potential candidate as an absorbent for large organic molecules or biomolecules.

**Acknowledgement** The authors gratefully acknowledge the financial support of the National Nature Science Foundation of China (no. 50573030).

**References**

1. Elliott J, Bond G, Tombe J (1980) J Appl Cryst 13:618
2. LeGeros R (1965) Nature 206:403
3. Thompson JB, Kindt JH, Drake B, Hansma HG, Morse DE, Hansma PK (2001) Nature 414:773

4. Ozin GA, Coombs N, Davies JE, Perovic DD, Ziliox M (1997) *J Mater Chem* 7:1601
5. Dorozhkin SV (2009) *J Mater Sci* 44:2343. doi:10.1007/s10853-008-3124-x
6. Karlinsky RL, Mackey AC (2009) *J Mater Sci* 44:346. doi:10.1007/s10853-008-3068-1
7. Krylova E, Ivanov A, Orlovski V, El-registan G, Barinov S (2002) *J Mater Sci Mater Med* 13:87
8. Ono I, Yamashita T, Jin HY (2004) *Biomaterials* 25:4709
9. Kandori K, Tsuyama S, Tanaka H, Ishikawa T (2007) *Colloids Surf B* 58:98–104
10. Groot KD (1984) *Bioceramics of Calcium Phosphate*. CRC, Boca Raton
11. Torrent-Burgues J, Torrent-Burgues J, Boix T, Fraile J, Rodriguez-Clemente R (2001) *Cryst Res Technol* 36:1075
12. Lagaly G, Beneke K, Dietz P, Weiss A (1974) *Angew Chem Int Ed Engl* 13:819
13. Prevot V, Forano C, Besse JP (2005) *Chem Mater* 17:6695
14. Choudary BM, Jaya VS, Reddy BR, Kantam ML, Rao MM, Madhavendra SS (2005) *Chem Mater* 17:2740
15. Jiang JQ, Xu YL, Quill K, Simon J, Shettle K (2007) *Ind Eng Chem Res* 46:4577
16. Swanson CH, Shaikh HA, Rogow DL, Oliver AG, Campana CF, Oliver SR (2008) *J Am Chem Soc* 130:11737
17. Ogawa M, Ide Y, Mizushima M (2010) *Chem Commun* 46:2241
18. Wei M, Pu M, Guo J, Han JB, Li F, He J, Evans DG, Duan X (2008) *Chem Mater* 20:5169
19. Xiang X, Hima HI, Wang H, Li F (2008) *Chem Mater* 20:1173
20. Thyveetil MA, Coveney PV, Greenwell HC, Suter JL (2008) *J Am Chem Soc* 130:4742
21. Bhattacharjee S, Dines TJ, Anderson JA (2008) *J Phys Chem C* 112:14124
22. Chuang YH, Tzou YM, Wang MK, Liu CH, Chiang PN (2008) *Ind Eng Chem Res* 47:3813
23. Begu S, Aubert-Pouessel A, Polexe R, Leitmanova E, Lerner DA, Devoisselle JM, Tichit D (2009) *Chem Mater* 21:2679
24. Ng SX, Guo J, Ma J, Loo SC (2010) *Acta Biomater* 6:3772
25. Zhang JX, Fujiwara M, Xu Q, Zhu YC, Iwasa M, Jiang DL (2008) *Microporous Mesoporous Mater* 111:411
26. Yuan ZY, Liu JQ, Peng LM (2002) *Langmuir* 18:2450
27. Schmidt SM, McDonald J, Pineda ET, Verwilt AM, Chen Y, Josephs R, Ostafin AE (2006) *Microporous Mesoporous Mater* 94:330
28. Ikawa N, Oumi Y, Kimura T, Ikeda T, Sano T (2006) *Chem Lett* 35:948
29. Kamitakahara M, Okano H, Tanihara M, Ohtsuki C (2008) *J Ceram Soc Japan* 116:481
30. Yao J, Tjandra W, Chen YZ, Tam KC, Ma J, Soh B (2003) *J Mater Chem* 13:3053
31. Zhao YF, Ma J (2005) *Microporous Mesoporous Mater* 87:110
32. Guo HF, Ye F, Zhang HJ (2008) *Materials Letters* 62:2125
33. Coelho JM, Moreira JA, Almeida A, Monteiro FJ (2010) *J Mater Sci Mater Med* 21:2543
34. Tanaka H, Watanabe T, Chikazawa M, Kandorib K, Ishikawa T (1998) *Colloids Surfaces A* 139:341
35. Soten I, Ozin GA (1999) *J Mater Chem* 9:703
36. Zhang SH, Wang YJ, Wei K, Liu XJ, Chen JD, Wang XD (2007) *Mater Lett* 61:1341
37. Liu C, Ji XJ, Cheng GX (2007) *Appl Surf Sci* 253:6840
38. Ikawa N, Hori H, Kimura T, Oumi Y, Sano T (2008) *Langmuir* 24:13113
39. Ikawa N, Oumi Y, Kimura T, Ikeda T, Sano T (2008) *J Mater Sci* 43:4198. doi:10.1007/s10853-008-2602-5
40. Cheng GX, Liu C (2002) *Mater Chem Phys* 77:359
41. Jack KS, Vizcarra TG, Trau M (2007) *Langmuir* 23:12233
42. Vallet-Regí M, González-Calbet JM (2004) *Progress Solid State Chem* 32:1
43. Doat A, Fanjul M, Pellé F, Hollande E, Lebugle A (2003) *Biomaterials* 24:3365
44. Milev AS, Kannangara GS, Wilson MA (2004) *Langmuir* 20:1888
45. Lagaly G (1976) *Angew Chem Int Ed Engl* 15:575
46. Snyder RG, Strauss HL, Elliger CA (1982) *J Phys Chem* 86:5145
47. MacPhail RA, Strauss HL, Snyder RG, Elliger CA (1984) *J Phys Chem* 88:334
48. Vaia RA, Teukolsky RK, Giannelis EP (1994) *Chem Mater* 6:1017
49. Kitaigorodskii AI (1973) *Molecular crystals and molecules*. Academic, New York
50. Huo QS, Margolese DI, Ciesla U, Demuth DG, Feng PY, Gier TE, Sieger P, Firouzi A, Chmelka BF, Schüth F, Stucky GD (1994) *Chem Mater* 6:1176